9-2013

The Role of Mechanically Induced ERK Phosphorylation in Stem Cell Adipogenesis

Daniel E. Menter
University of Nebraska-Lincoln, dmenter@huskers.unl.edu

The Role of Mechanically Induced ERK Phosphorylation in Stem Cell Adipogenesis

By

Daniel E Menter

A THESIS

Presented to the Faculty of

The Graduate College at the University of Nebraska

In Partial Fulfillment of Requirements

For the Degree of Master of Science

Major: Mechanical Engineering and Applied Mechanics

Under the Supervision of Professor Jung Yul Lim

Lincoln, Nebraska

September, 2013

The Role of Mechanically Induced ERK Phosphorylation in Stem Cell Adipogenesis

Daniel E Menter, M. S.

University of Nebraska, 2013

Adviser: Jung Yul Lim

Mechanical cell stimulation has only recently been highlighted for its ability to direct cell function and fate. The development of techniques to apply controlled mechanical stimulation to cells has allowed researchers to examine the effects of forces on cell behavior. These studies have shown that cells, and in particular, stem cells are very sensitive to mechanical stimuli. While the potential impact of mechanical forces has been demonstrated by these studies, there have not been many studies that compare the differing effects of stimulation profiles and methods. Further, molecular mechanosensing mechanisms have not been identified. In this work, we compared the effects of cyclic tensile stretch and fluid flow induced shear on mesenchymal stem cell (MSC) adipogenesis. We also implicated extracellular signal-regulated kinase (ERK) phosphorylation as a molecular mechanism involved in both cases.

To test mechanical control of MSC adipogenesis, C3H10T1/2 murine MSCs were exposed to cyclic equibiaxial tensile stretch at 10% strain or 20 dyne/cm^2 of fluid flow induced shear and induced to differentiate. For this, Flexcell FX-5000 cell stretching device and Flexcell Streamer fluid flow devices were used. Interestingly, lipid accumulation, a marker of MSC adipogenesis, was suppressed by both mechanical stretch and flow shear. Also, genetic markers for MSC adipogenic

commitment (PPARγ, aP2, and C/EBPα) were down regulated by cell stretch. We observed as a potential mechanotransduction mechanism that both stimulation methods induced significant ERK1/2 phosphorylation in MSCs. Furthermore, both stretch and flow induced mechanical suppression of MSC adipogenesis was deteriorated in the presence of PD98059, an established pharmacological ERK inhibitor. Combined, these results indicate that cell stretch and fluid flow suppress adipogenic commitment and differentiation of MSCs, potentially via the mechanical activation of ERK signaling. While more comparisons of varying regimens are required, our data suggests that both cell stretch and fluid flow have potential to down regulate MSC adipogenesis and may share a similar cell mechanotransduction mechanism such as ERK. Further, inhibiting MSC adipogenesis via mechanical cues may provide new insights for obesity research.

Acknowledgements

First, I would like to acknowledge my advisor Dr. Jung Yul Lim for his guidance in designing, executing, and communicating this project. His technical expertise in cell mechanotransduction and materials engineering have been assets to my academic development and his experience with study design and communication have been a great source of help and reference.

I would like to thank Dr. Jung Yul Lim, Dr. Linxia Gu, and Dr. Sangjin Ryu for serving on my thesis committee and for their assistance and constructive comments.

I would like to thank Dr. Jeong Soon Lee, Ligyoem Ha and all of my lab members for their technical support.

Last but not least, I would like to thank my wife and our family for their continuous moral support and encouragement throughout my time at the University of Nebraska.

Table of Contents

List of Figures

Chapter 1 : Introduction

Obesity is well recognized as a major driver of health care costs in the United States due to the wide range of health problems associated with it. Over 90 million Americans can be categorized as obese including 12 million children according to the Centers for Disease Control and Prevention (Ogden, et al., 2012). The treatment of obesity related diseases cost 150 billion dollars in 2008 (Finkelstein, et al., 2009). As more of our economy becomes involved in the support and delivery of healthcare, the importance of slowing the growth of obesity is of utmost importance. Unfortunately not enough is known about the molecular mechanisms that control cellular adipogenesis and as a result, obesity. This study on how to control stem cell adipogenesis may help to fill that knowledge gap.

Literature Review

On a clinical level, obesity is characterized by a body mass index of greater than 30 in adults. As an individual reaches and exceeds that level, the incidence of heart disease, diabetes, liver steatosis, and several cancers rises dramatically (Cornier, et al., 2008; Shoham and Gefen, 2012). On a population scale, the most effective measures have focused on diet and exercise. However the complex interactions of the cellular processes that control the risk for and development of obesity are not well understood. On a cellular level, obesity is identified by excessive growth and hypertrophy of adipocytes through recruitment of new pre-adipocytes and mitotic clonal expansion of preadipocytes (Tang, et al., 2003; Yu, et al., 1997). While we know how to characterize

adipogenesis and obesity, not much is known about the underlying cellular and/or molecular mechanisms. As a result, there has been increased interest in the mechanisms by which cellular adipogenesis occurs and how to inhibit such processes. Many studies have focused on biochemical (soluble) cues, including bone morphogenetic protein (BMP) 4 (Bowers and Lane, 2007) and retinoic acid (Lee, et al., 2011), in regulating cellular adipogenesis. Interestingly, it was demonstrated that BMP4, which was originally named based on its ability to induce osteoblastic differentiation and bone development, is also strongly involved in the preadipocytic commitment of mesenchymal stem cells (MSCs) (Bowers and Lane, 2007). On the other hand, retinoic acid has an inhibitory effect on the BMP4 induction of stem cell commitment toward adipogenesis if treated during the BMP4 exposure period, as was reported in our group's previous study (Lee, et al., 2011). The complex interdependency of these signaling pathways on cellular adipogenesis has complicated the isolation of relevant molecular parameters in studying obesity. Recently, as an unconventional approach, a few studies have begun to probe non-soluble, e.g., mechanical, control of cellular adipogenesis and therefore obesity (Shoham and Gefen, 2012). This may provide entirely new concepts to deal with obesity and related metabolic diseases.

Mechanical Control

Recently there has been increased interest in mechanophysical control of cell behavior. Studies have been devised to probe the effect of substrate topography, cell micro-confinement, forced cell alignment, mechanical stretch, fluid flow, and hydrostatic pressure on cell behavior. The mechanophysical signals do not always produce similar cell outcomes. For example, it was demonstrated that cyclic pressure and fluid flow differentially affect the actin network of osteoblasts, causing vastly different responses in subsequent signaling events (Gardinier, et al., 2009).

A review article by Bodle, Hanson, and Loboa (2011), presented in figure 1-1, well summarized the differing effects of physical stimuli on cell morphology and cytoskeletal structure. They reviewed evidence that fluid flow induced shear deforms the apical surface of cells and causes ion channel activity change and cytoskeletal alignment (figure 1-1 a). Tensile strain, which is majorly sensed via integrin focal cell adhesion proteins, also induces ion channel activation (figure 1-1 b). Compressive strain on the other hand compacts the cytoskeleton (figure 1-1 c). The electrical field, while not strictly belonging to the mechanical cues, induces the alignment of the cytoskeleton perpendicular to the field (figure 1-1 d). Finally, substrate compliance is shown to limit cell spreading and cause integrin mediated changes in cell behavior (figure 1-1 e).

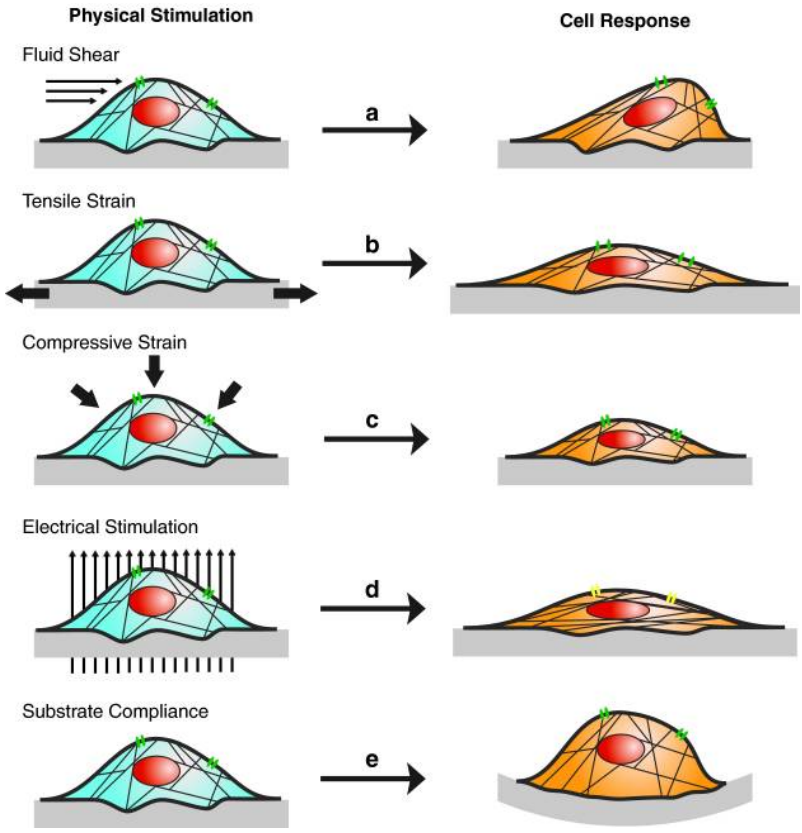

Figure 1-1 Cells respond differently to different mechanical stimuli (Bodle, et al., 2011)

These observations suggest that even in the case where different loading methods produce similar changes in cell behavior, it may be achieved through different mechanisms. It is also likely that the same loading method may produce versatile effects on cell behavior depending on cell sources/lines. For example, cyclic compression has been shown to enhance chondrogenic gene expression in human MSCs (Campbell, et al., 2006) as well as osteoblastic genes in rat MSCs (Liu, et al., 2009). Also, MLO-Y4 osteocytic cells and MC3T3-E1 osteoblastic cells responded differently to fluid flow stimulations depending on oscillatory and unidirectional flows (Ponik, et al., 2007). Even the same cell line displays differing levels of sensitivity to oscillatory and steady fluid flow in some cases (Case, et al., 2011). Combined, a more systematic investigation of the

effects of mechanical stimulation profiles on various cell types is necessary to isolate the optimal regimen for control of cells.

Fluid flow

Fluid flow has been proposed as a potential regulator of cell function for many years. Early efforts focused on biomimetics in an attempt to develop flow bioreactors for regenerative medicine purposes and in particular functional vascular tissue (Radisic, et al., 2007). With recent advances in engineering tools including finite elemental analysis, one can more accurately analyze the minute differences in forces and perform systematic studies. This allows us to control more of the variables and isolate the effect of differing levels and profiles of shear.

It was shown that fluid flow influences many cytosolic cell signaling pathways, including the extracellular signal-regulated kinases (ERK) pathway, the cyclo-oxygenase (COX) pathway, and the nitric oxide synthase pathway (Kapur, et al., 2003). These results suggest that fluid flow stimuli may have many different effects on cells by triggering several independent (or inter-correlated) mechanistic cascades. They also showed that ERK phosphorylation is required for fluid flow regulation of osteoblastic DNA synthesis and alkaline phosphatase production. An interesting side result was the discovery that an increase in integrin β1 expression was not required for shear stress induced increases in proliferation and differentiation. Their work with the COX and nitric oxide pathways specifically suggest that there may be multiple pathways for the

same end cell phenotype to be achieved. In this case, both ERK-dependent and ERK-independent pathways were implicated in fluid flow control of osteoblastic differentiation (Kapur, et al., 2003). In another study, it was demonstrated that the nitric oxide pathway responds differentially to flow oscillation frequency, suggesting that there may be differing morphogenic and phenotypic responses based on the flow profile and regimen (Mullender, et al., 2006).

Regulation of the COX-2 and ERK pathways was also shown to be tightly regulated by protein kinase A (PKA). Fluid flow induction of COX-2 expression is independent of prostaglandin, while significant crosstalk between ERK and PKA pathways may be occurring under fluid flow (Wadhwa, et al., 2002). Such a crosstalk makes it difficult to isolate the exact pathway that is being stimulated under flow and responsible for specific terminal cell behavior.

In order to design the systematic studies necessary to isolate the different effects of flow shear forces, one must have a working knowledge of fluid mechanics. The shear stress produced by fluid flow can be approximated based on the flow profile. The flow profile, in large part, depends on whether it is laminar or turbulent. This is determined by the Reynolds number (*Re*) defined by $Re = \rho \frac{Vh}{\mu}$, where ρ is the fluid density, V is the fluid velocity, h is the channel height, and μ is the dynamic viscosity of the fluid. The Flexcell streamer system, used in this study for the fluid flow stimulation of cells, has a flow channel height of 0.05 cm. The flow media (serum starved cell culture media, 0.5% serum) has an approximate viscosity of 7.8×10^{-3} dyne·s/cm^2 and density of 1 g/cm^3.

Based on the transition from laminar to turbulent flow occurring at a Reynolds number of 2300 we can approximate the transition velocity at 359 cm/s or about 2.6 L/min for our Streamer device. Since the current study targeting 20 dyne/cm^2 of shear stress uses 0.73 L/min of volume flow rate (which is far below that transition limit), it may be assumed that the flow is laminar. Finite elemental analysis can be used to verify that cell confluence and height do not significantly affect the flow pattern (Salvi, et al., 2010), but was not performed in this study.

Once we have established that the flow is laminar, balancing Newton's second law gives us the velocity profile of $V(y) = \frac{6Q}{wh}(\frac{y}{h} - \frac{y^2}{h^2})$ where y is the distance from the channel bottom, Q is the volume flow rate, w is the channel width, and h is the total channel depth. The shear stress at the wall can be determined to be $\tau(y = 0) = \mu\frac{dV}{dy}(y = 0) = \mu\frac{6Q}{wh^2}$. This allows us to accurately control the shear stress to which cells seeded at the wall of the chamber are exposed to by controlling the volume flow rate.

Stretch

Another physiologically relevant mechanical cue is tensile stretch. Studies have demonstrated the potential of mechanical cell stretch to promote stem cell differentiation toward the osteoblastic fate. For example, bone marrow MSCs showed increased alkaline phosphatase activity and core binding factor α1 (Cbfa1) mRNA expression, both of which are typical osteogenic markers, when exposed to cell stretching below 5%

strains (Koike, et al., 2005). Also, mechanical stretching at 2-10% strains induced increased expression in several transcription factors and genes (Runx2, FosB, Ets-1) that play a crucial role in the differentiation of MSCs to osteoblasts (Haasper, et al., 2008; Qi, et al., 2008)The increase of Cbfa1 in human MSCs under stretching resulted in increased alkaline phosphatase activity and bone-like mineralization (Huang, et al., 2009). More physiologically, MSCs stretched within 3D collagen scaffold displayed increased osteoblastic differentiation under 10% strains (Sumanasinghe, et al., 2008). Also, the induction of MSCs toward skeletal muscle phenotype and ligament and tendon via mechanical stretch has been attempted in functional tissue engineering (Benhardt and Cosgriff-Hernandez, 2009; Nieponice, et al., 2006) Together, it is now recognized that mechanical stretch has the potential to induce MSC differentiation toward a musculoskeletal fate such as osteogenesis and skeletal myogenesis, however the regulatory mechanosensing mechanisms have yet to be revealed.

Stretch has been also shown to regulate the proliferation of MSCs and may be able to induce commitment to a smooth muscle lineage without the addition of growth factors (Ghazanfari, et al., 2009). It was also shown that stretch prevents the cross-differentiation of C2C12 myoblasts into adipocytes (Akimoto, et al., 2005). This was shown to be at least partially dependent on the activation of the Wnt signaling pathway.

More relevant to this study, it was shown that mechanical cell stretching may inhibit the adipogenesis of preadipocyte cells (Tanabe, et al., 2004). Note that they used 3T3-L1 preadipocytes but and did not test MSC adipogenesis. It was also shown that cell stretch could downregulate the expression of peroxisome proliferator-activated receptor γ

(PPARγ) in bone stromal cells (David, et al., 2007), thus decreasing their adipogenesis. Note that PPARγ is one of the key adipogenic transcription factors. This regulatory power was involved in the control of switching of mesenchymal stem cell fate from adipogenesis to osteogenesis. They further showed that stretching could overcome the effect of Rosiglitazone, a PPARγ agonist that increases adipogenesis, and thus induced their osteogenesis. In the presence of GW9662, a PPARγ antagonist, the stretch effect was attenuated. These observations demonstrated a potential interplay of mechanical and biochemical signals in stem cell fate decision.

In regard to the effects of stretch regimens, just as in the case of fluid flow, not all stretch is created equal. For example, a study comparing equiaxial stretch with uniaxial stretch found that while the genes for α-actin and SM-22α were upregulated by uniaxial stretch, they were downregulated by equiaxial stimulation (Park, et al., 2004). Other potential parameters to consider are the strain magnitude, the frequency and length of the stretching periods, insertion of resting period or not, and the stage of the cells life cycle stimulation occurs at.

BMP4

BMPs are members of the transforming growth factor β superfamily that were initially identified for their ability to induce ectopic bone formation (Urist, 1965). It has also been demonstrated that BMPs are implicated as important regulators of many other developmental processes including those of the heart, nervous system, cartilage, liver,

and kidney (Bandyopadhyay, et al., 2013; Hogan, 1996) BMP-2, -4, and -7 are well known for their importance to the development of osteoblasts and bone formation and have recently been the subject of investigation as to their role in cell mechanotransduction pathways (Yang, et al., 2010).

Recently, as noted above, BMP4 has also been established as an important regulator of mesenchymal stem cell commitment to a preadipocyte lineage (Bowers and Lane, 2007). When proliferating C3H10T1/2 cells are treated with BMP4, they show preadipocyte commitment and can be further treated with adipogenic hormonal inducers to acquire a terminal adipocyte phenotype. Recent studies have also suggested that BMP4 may play a role in directing MSCs to white adipose tissue at the expense of brown adipogenesis (Modica and Wolfrum, 2013). As an advanced adipogenesis cell model for obesity study, this study focused on the MSC adipogenesis model, with or without BMP4, instead of using a conventional preadipocytic 3T3-L1 cell line. As noted above, we have shown that retinoic acid could inhibit BMP4 induced MSC adipogenesis and this may be accomplished through the downregulation of BMP4-Smad/P38MAPK signaling (Lee, et al., 2011).

ERK Phosphorylation

ERK phosphorylation has been widely viewed as a potential signaling pathway for many mechanotransduction studies. It has been shown that ERK is phosphorylated in response to fluid flow (Young, et al., 2009), cyclic stretch (Tanabe, et al., 2004), pulsatile

hydrostatic pressure (Kim, et al., 2007), and simply the topography of the substrate (Hamilton and Brunette, 2007). The upstream and downstream effectors of ERK pathways are not fully known. Some of the known interactions in the ERK1/2 pathway are shown in figure 1-2 as well as other pathway known to be involved in

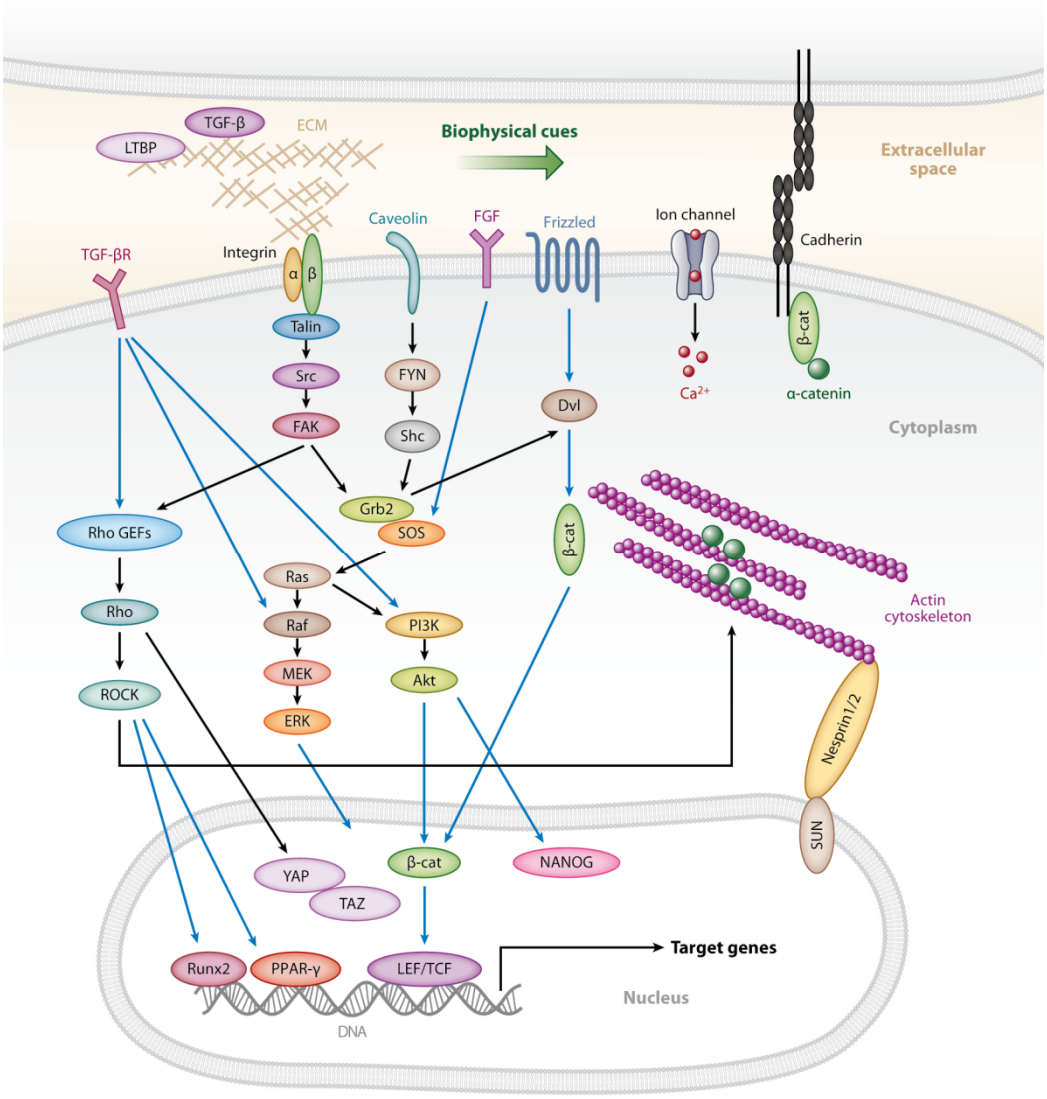

Figure 1-2 Transduction pathways of mechanical signals. (Sun, et al., 2012)

mechanotransduction including the Rho/ROCK and β-Catenin pathways. Specifically, biophysical cues are detected by membrane bound proteins including integrin. This

signal is then conveyed along the pathway through the Rous sarcoma oncogene cellular homolog (Src) and focal adhesion kinase (FAK) families and into the Ras-Raf-MEK-ERK phosphorylation cascade. Regardless of the specific steps in the pathway, it is known is that ERK phosphorylation may play a pivotal role in the regulation of many cell functions including cell proliferation and differentiation.

It is relatively well established that mechanically induced ERK activation may increase cell number through proliferation (Riddle, et al., 2008). Control of cell differentiation by mechanically induced ERK activation includes stem cell commitment to chondrogenesis or osteogenesis under cyclic compression (Palaez, et al., 2012), control of early osteogenesis by hydrostatic pressure (Liu, et al., 2009), and stretch inhibition of adipogenesis (Lee, et al., 2012).

Research Objectives

The objectives of this study were multiple. The first objective was to test the effect of different mechanical stimulation methods on MSC adipogenesis. This was done by conducting experiments that applied cell stretch and fluid flow during early MSC differentiation and assessed MSC adipogenic differentiation by various means eight to ten days later. Secondly, we sought to determine the cellular mechanosensing mechanism responsible. Particularly, we suspected ERK1/2 phosphorylation is at least partially responsible for the adipogenesis inhibitory effects of mechanical stimulation. To confirm this, a pharmacological inhibitor was used to inhibit ERK activity and the proposed mechanical cell stimulation experiments were repeated. Finally, this research aimed to compare the effect of stretch and shear forces in controlling MSC adipogenesis in the context of dealing with obesity.

Organization of Thesis

Chapter one focuses on the background knowledge required to understand the experimental parameters and theses. Chapter two is about the design and results of the stretch experiment. Chapter three contains the design and results of the fluid flow experiment. Chapter four is a discussion of the findings. Chapter five presents our conclusions and probes the implications of this study.

Chapter 2 : Stretch

Experimental Design

The stretch portion of this experiment follows a design describe below. First we test whether stretch decreases MSC adipogenic commitment induced by BMP4 via assessing Oil Red O lipid staining and gene expression. Next we examine if stretch increases ERK phosphorylation and compare with BMP4 treatment alone case. Finally we test the effect of blocking ERK activation by PD98059 on the stretch induced MSC adipogenesis inhibition.

A general overview of the experiment can be seen in figure 2-1. Four days prior to adipogenic induction, cells were seeded on collagen coated silicon membranes. The cells were then subjected to stretch while being treated with BMP4. After four days of BMP4 and stretch treatment, cells were exposed to adipogenic induction media for 48 hours. Finally the cells were incubated in adipogenic maintenance media for an additional six days (see media additives in cell culture section). Lipid accumulation was then assessed using Oil Red O staining and isopropanol extraction.

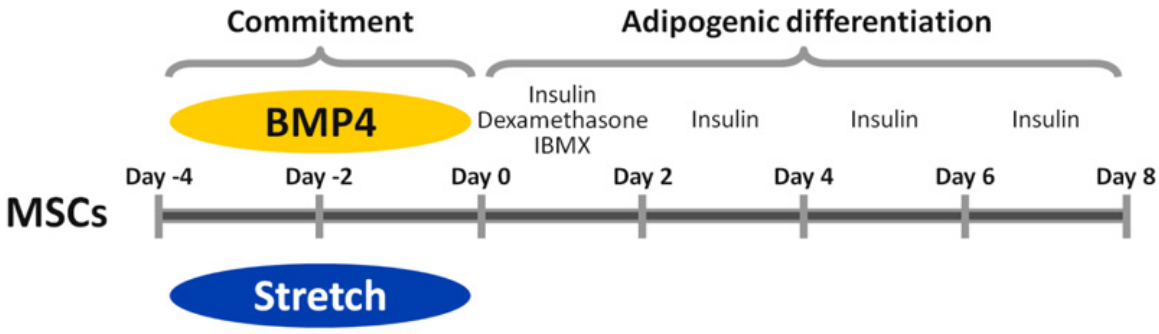

Figure 2-1 Experimental overview: Stretch

Mechanical Stimulation

Cells were subjected to stretch during the BMP4 pretreatment period to examine the mechanical control of BMP4 induction. The FX-5000 tension system (Flexcell) was used to stretch the collagen coated silicon membrane on which cells are cultured. A computer-controlled system of valves allowed for precise control of vacuum pressure on the membrane to achieve required membrane deformation (and thus required strain).

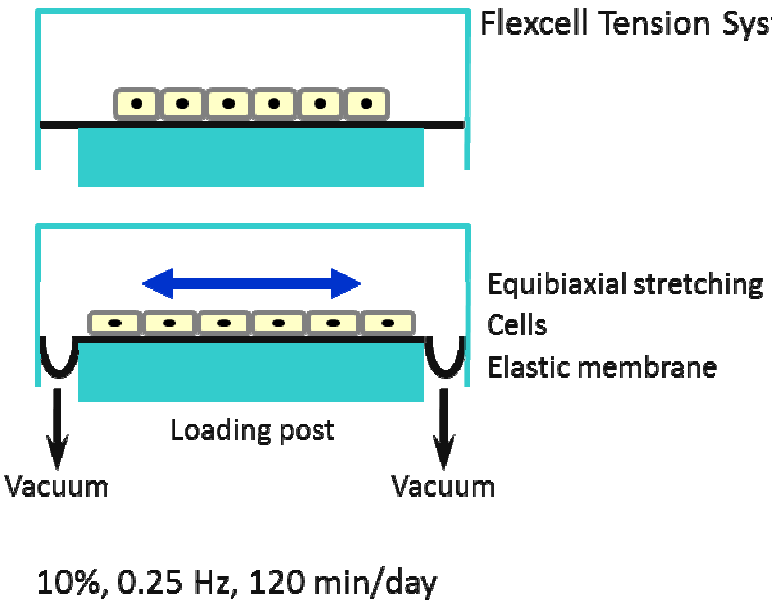

Figure 2-2 Stretch mechanism

The pressure causes the elastic membrane to be pulled down against a silicone lubricant smeared loading post and generate precise membrane deformations as in figure 2-2. Appropriate selection of elastic membrane and the loading post enabled equiaxial tensile stretching of the cells at a predetermined strain and stretch frequency. We applied cyclic equiaxial elongation (10% strain at 0.25 Hz) for 120 min/day for the 4 days of the BMP4 pretreatment period. Using multiple six well plates at the same time allowed the

simultaneous stimulation of enough samples and groups to achieve significant results.

Figure 2-3 Six well plate with silicone membrane and posts

The complete setup with a six well plate on the circular loading posts (for equiaxial motion) seated in a rubber gasket can be seen in figure 2-3. The plates and suction mechanism were placed inside an incubator at 37^{o} C and 5% CO_2. This allowed us to perform cell stretching tests at normal cell culture conditions.

Cell Culture

C3H10T1/2 MSCs were maintained in Dulbecco's Modified Eagle Medium (DMEM) supplemented with 10% fetal bovine serum (FBS) and 1% penicillin-streptomycin. For tests, cells were seeded on collagen-coated silicone membranes (Bioflex 6-well plate, Flexcell) and cultured to confluence which took four days (figure 2-1). Once confluent, cells were induced to differentiate using adipogenic differentiation media consisting of maintenance media supplemented with 10 µg/ml insulin, 1 µM dexamethasone, and 0.5 µM methylisobutylxanthine for two days before being changed to adipogenic maintenance media (10 µg/ml insulin only). The cells were kept for an

additional 6 days, changing the maintenance media every two days. The groups containing BMP4 were cultured in much of the same manner however, the media was supplemented with 50 ng/ml recombinant BMP4 (R&D Systems) during the 4 days of proliferation prior to adipogenic induction.

Data Collection

Lipid accumulation was assessed using Oil Red O staining and isopropanol extraction. The standard protocol as was published from the lab (Lee, et al., 2011) was used. First, cells were fixed by immersion in 10% formalin for 60 minutes. Following washing in distilled water and rinsing with 60% isopropanol, fixed cells were stained with 0.5% Oil red O solution by immersion for 10 minutes. Following several washes with distilled water, the samples were photographed while submerged. Finally, the lipid was extracted using isopropanol and the optical absorbance at 570 nm was measured using a spectrophotometer (BioTek) to quantify the amount of lipid synthesis.

To assess the phosphorylation of ERK1/2 protein, western immunoblotting was used as in our published protocol (Lee, et al., 2011). Briefly, immediately after BMP4/stretch stimulation, cells were scraped off into chilled centrifuge tubes. Protein was then harvested by lysing them with buffer solution consisting of distilled water supplemented with 0.1 % v/v Triton X-100, 1% v/v Tris-EDTA, 1% v/v protease inhibitors (Calbiochem), and 0.2 μM Na3VO4. Protein was then quantified by dying and measuring the absorbance at 595 nm. Defined amounts of protein were fractionated by

electrophoresis in a polyacrylamide gel and transferred to a polyvinylidene diflouride film. Following blocking with 5% skim milk in TBS-T (1-mM Tris, 150 mM NaCl, 0.05% Tween 20), the blots were exposed to primary antibodies for ERK1/2 and phosphorylated ERK1/2 (Santa Cruz) diluted in 5% skim milk in TBS-T overnight. The blots were then washed and treated with a secondary antibody conjugated to horseradish peroxidase. The bands were visualized using electro-chemiluminescence (ECL). The band intensity of phosphorylated ERK1/2 was quantified using imageJ and normalized to that of total ERK1/2 protein. GAPDH was also used as a loading control.

To evaluate adipogenic gene expression, after 24 hours of induction, total RNA was extracted and quantitative RT-PCR was performed. Expressions of PPARγ, CCAAT/enhancer binding protein alpha (C/EBPα), and adipocyte protein 2 (aP2) were measured as previously described (Lee, et al., 2008). GAPDH was used as a loading control. Trizol (Invitrogen) was used to lyse the cells, and the RNA was extracted by first treating with chloroform to precipitate and separate out the non-genetic material and DNA followed by isopropanol to generate an RNA pellet. The RNA was then dissolved in diethylpyrocarbonate (DEPC) treated water. One microgram of RNA was converted to cDNA using an RT premix kit (Bioneer) according to the manufacturer's directions. cDNA was then amplified by polymerase chain reaction, separated by electrophoresis and visualized using ethidium bromide.

Analysis of Data

Data was analyzed using InSTAT 3 statistic software. Statistical significance was established using one way analysis of variance (ANOVA) followed by post-hoc tests.

Results

On day 1 (figure 2-1), commitment of MSCs to pre-adipocytes was assessed using RT-PCR. As can be seen in figure 2-4, BMP4 significantly increased the commitment of C3H10T1/2 MSCs to the adipocyte lineage as seen by an increase in key adipogenic transcription factor expression, i.e., PPARγ, C/EBPα and aP2.

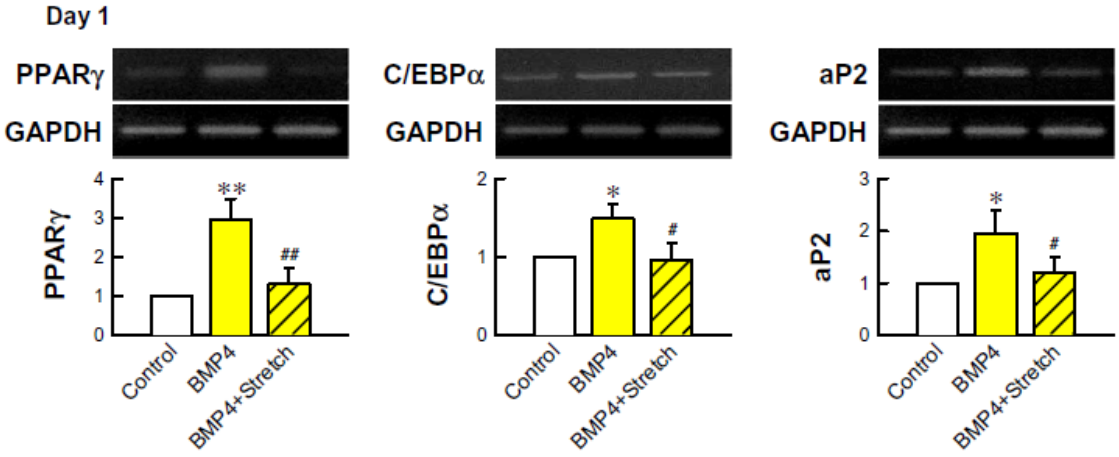

Figure 2-4 BMP4 induced adipogenic mRNA expression was significantly decreased by cell stretching. Quantitative RT-PCR data normalized to the control samples. Comparison with the control (*, **) and with BMP4 (#, ##) shown at $p < 0.05$ (*, #) and $p < 0.01$ (, ##)**

Interestingly, such BMP4 induced increase in adipogenic gene was almost entirely blocked by stretch stimulation during the BMP4 treatment period. All differences between BMP4 treatment group and BMP4 plus stretch treated group were significant. Lipid staining, which is a marker of terminal adipogenesis, showed the same trends on day 8 (figure 2-5). BMP4 treated cells show dramatically higher lipid accumulation than either untreated control cells or cells treated with BMP4 and subjected to four days of stretching. Stretch did not entirely block the deposition of lipid however.

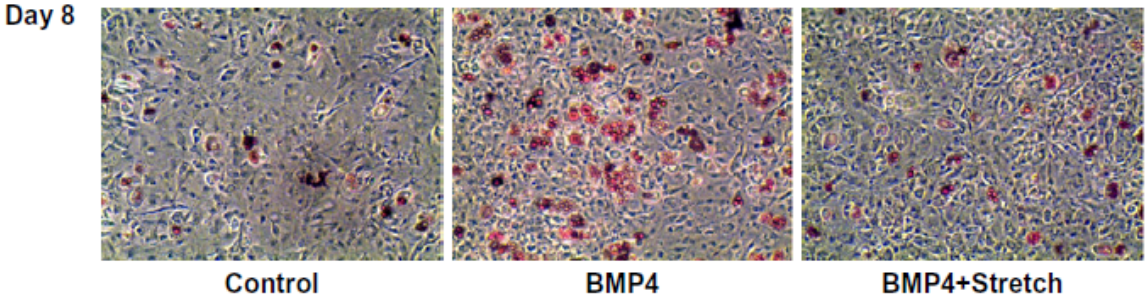

Figure 2-5 BMP4 increased lipid accumulation, which effect was significantly reduced by cell stretching (oil red O staining).

ERK activation may be a potential regulatory step in the commitment of mesenchymal stem cells. To implicate this pathway in C3H10T1/2 cells, ERK phosphorylation was measured at various time points using western blot. In the case of

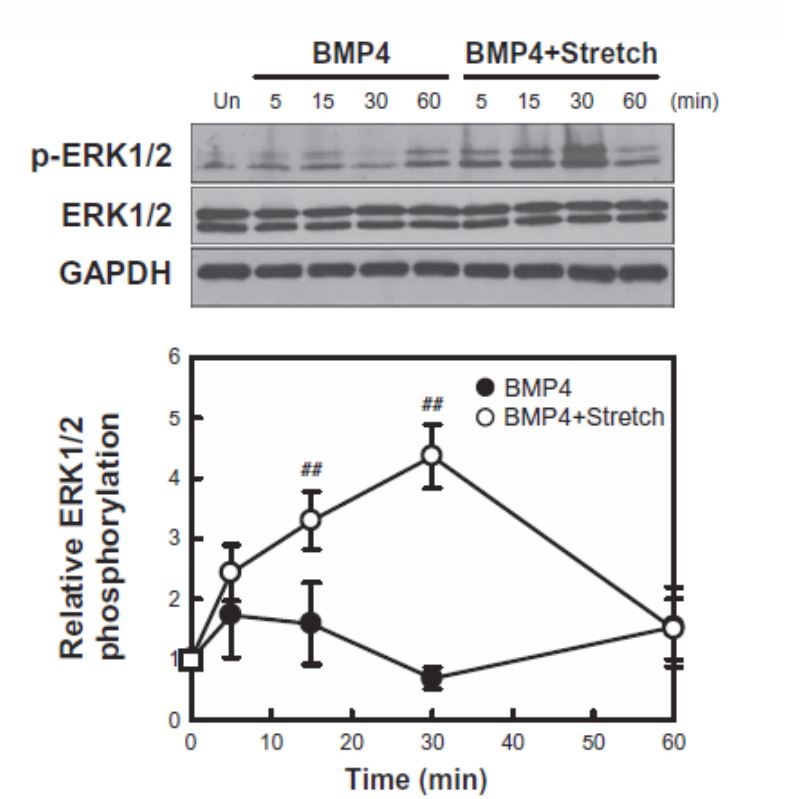

Figure 2-6 ERK1/2 phosphorylation (p-) was quantified, normalized with total protein, and presented relative to untreated control (Un, empty square). ERK1/2 phosphorylation was significantly greater for BMP4 plus stretch at 15 and 30 min relative to BMP4 treatment

BMP4 treatment alone, ERK was not phosphorylated during the first hour (figure 2-6). When stretched, cells showed significant ERK1/2 phosphorylation which increased steadily over the first 30 minutes of stretch. At 15 and 30 minutes the stretch groups differed significantly from those treated with BMP4 alone. This can be seen in figure 2-6. This effect then decays over the next 30 minutes to that the increase is no longer significant one hour post stretch

To further test whether stretch induced ERK phosphorylation plays a mediatory role in stretch inhibition of MSC adipogenesis, the stretch assays were repeated with ERK inhibition. This was accomplished by pretreating cells 20 minutes prior to stretch

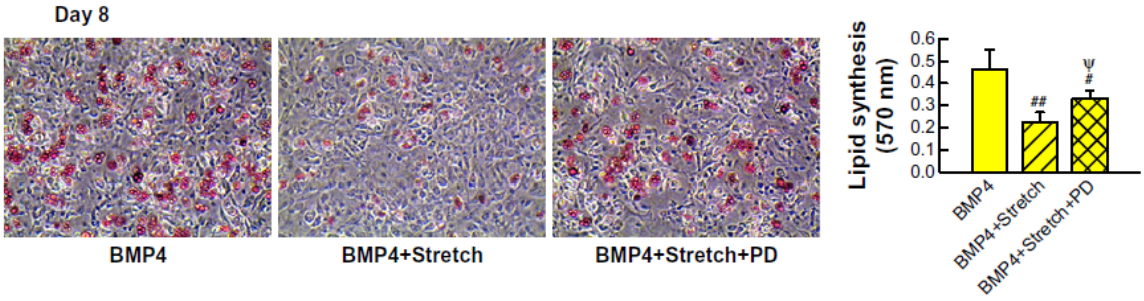

Figure 2-7 Cell stretching under ERK inhibition by PD98059 showed less significant decrease in lipid accumulation. Oil red O stained images and lipid quantification by spectrophotometer. Comparison with BMP4 (#, ##) and BMP4 plus stretch (ψ, ψψ) at $p < 0.05$ (#, ψ) and $p < 0.01$ (##).

with 20 μM PD98059, a known pharmacological blocker of ERK. As seen in figure 2-7, stretch suppression of BMP4 induced lipid accumulation was significantly deteriorated in the presence of ERK inhibition by PD98059 (PD). This suggests that stretch inhibition of MSC adipogenesis under BMP4 would be achieved through the stretch regulated ERK signaling. Adipogenic gene expressions shown in figure 2-8 display the same trend, i.e., disruption of stretch inhibition effects in the presence of ERK inhibition. Combined, these suggest that ERK may be involved in stretch regulation of BMP4-mediated

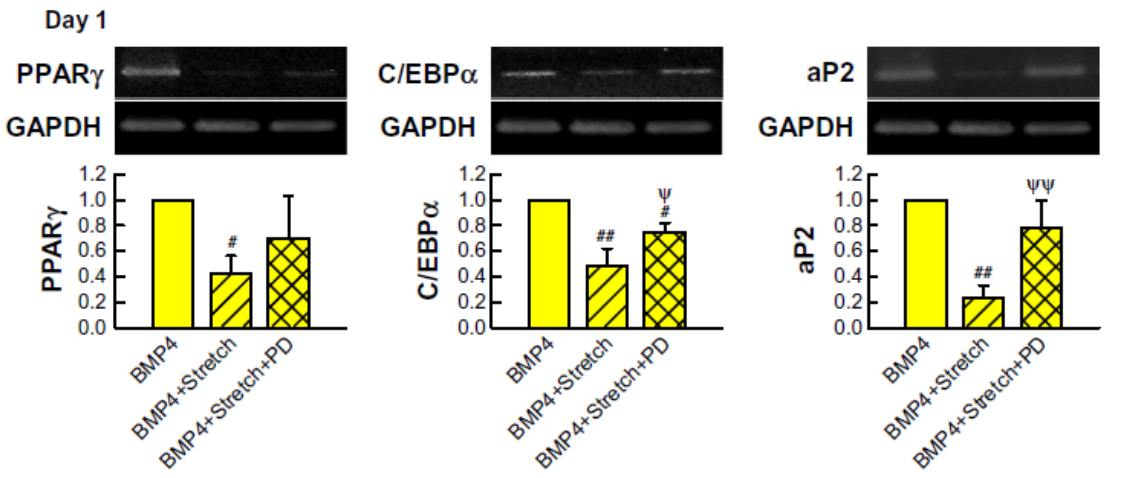

Figure 2-8 Stretch-induced decrease in adipogenic gene expression was less significant if stretch was applied under an ERK inhibitor, PD98059 (PD). Quantitative RT-PCR data shown with BMP4 sample as one. Comparison with BMP4 (#, ##) and BMP4 plus stretch (ψ, ψψ) shown at $p < 0.05$ (#, ψ) and $p < 0.01$ (##, ψψ).

adipogenic commitment and differentiation.

Chapter 3 : Fluid Flow

Experimental Design

As described in chapter one, fluid flow offers a great unknown of cellular mechanotransduction. In order to shed some light on fluid flow control of stem cell adipogenesis, this study first tests whether fluid flow stimulation can inhibit MSC adipogenesis. Next, we test if potential inhibitory effect by fluid flow is mediated by PPARγ by repeating the flow experiment in the presence of Rosiglitazone, a PPARγ agonist, and GW9662, a PPARγ antagonist. Finally, we test fluid flow triggering of ERK1/2 phosphorylation, and repeat the flow experiment in the presence of ERK inhibitor to reveal the role of ERK in directing fluid flow control of MSC adipogenesis.

The basic design of the experiment can be seen in figure 3-1 and is as follows: three days prior to fluid flow stimulation, cells were seeded on untreated, UV sterilized

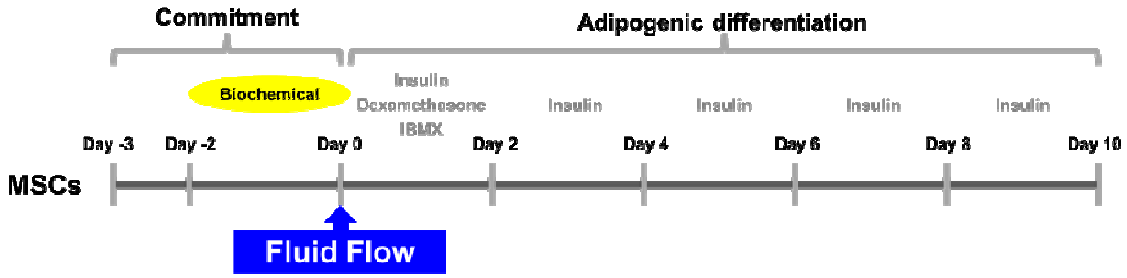

Figure 3-1 Experimental overview: Fluid Flow

glass slides. Following 24 hours of culture, cells were transferred to media containing the appropriate soluble biochemical factors. After 48 hours, cells were stimulated by fluid flow using serum starved (0.5% serum) flow media. After the flow period, cells were exposed to adipogenic induction media for 48 hours, and then to adipogenic maintenance

media for additional 8 days. Media was refreshed every 2 days during the differentiation period. Note that BMP4 was not used in fluid flow assays due to cost consideration.

Mechanical Stimulation

Experimental groups were subjected to flow shear on day 0 using the Flexcell Streamer system (Flexcell International). The schematic is shown in figure 3-2. We

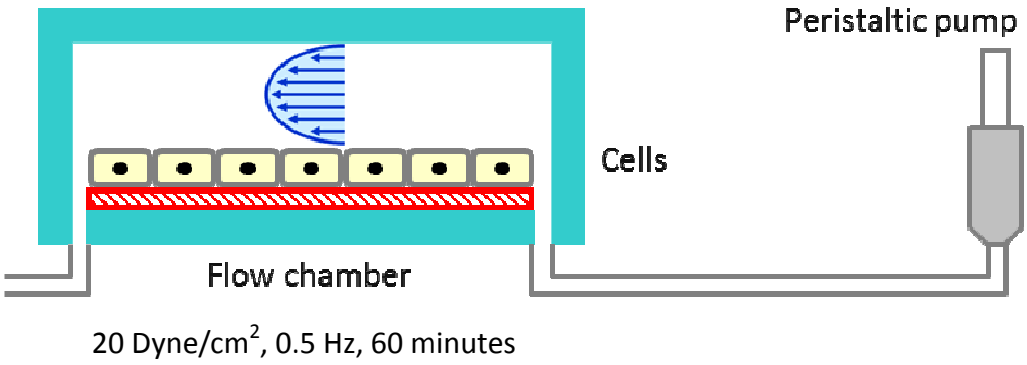

Figure 3-2 Fluid Flow mechanism

applied to the cells 20 dyne/cm^2 of fluid shear oscillating at 0.5 Hz for 60 minutes. This system uses a peristaltic pump to drive culture media across the cells at a constant volumetric flow rate. Upstream to the flow chamber are a series of bubble traps and the OsciFlow device (Flexcell International). The bubble traps dramatically decrease delamination and prevent the destruction of the samples due to unstable flow. The OsciFlow device will be explained in the next paragraph. Assuming laminar flow allows us to calculate the shear stress on the walls of the chamber with reasonable accuracy. As described in the introduction, we can then use the following formula for shear stress (τ) at

the wall resulting from steady flow between infinitely wide parallel plates: $\tau = \mu \frac{6Q}{wh^2}$ where μ is the fluid viscosity, Q is the volumetric flow rate, w is the width of the chamber, and h is the distance between the two plates. The volume flow rate and oscillation frequency were dynamically controlled by software provided by Flexcell International.

Oscillatory flows were generated by the OsciFlow device (a system of four valves as show in figure 3-3 B). The top right and bottom left valves open to allow flow one direction before closing and the other two valves open to send flow in the opposite direction. This allows the pump to continue to run in the same direction. Another advantage of the Flexcell streamer is its size. This can be seen in figure 3-3 A. It contains six slots for cell culture slides, allowing us to run a sufficient number of samples in a reasonable time period. This was especially helpful given the potential for issues

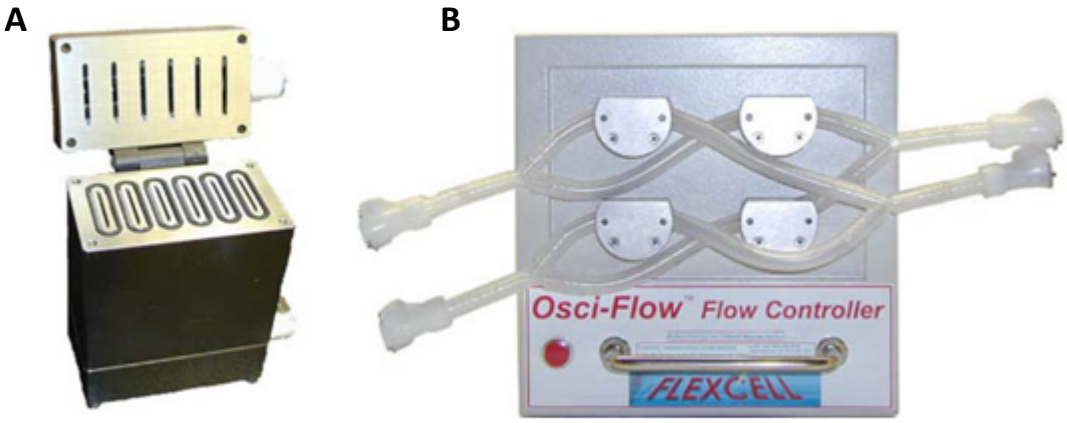

Figure 3-3 FlexCell Streamer and OsciFlow

with delamination and contamination. Note, to reduce the risk of contamination of the samples, all parts that come in direct contact with fluid or cells were autoclaved and the exterior parts sterilized using UV light

Cell Culture

The same MSCs used for stretch tests, C3H10T1/2 MSCs, were used for flow assays. Cells were maintained in DMEM with 10% FBS and 1% penicillin-streptomycin at 37^{o} C and 5% CO_2. For tests, cells were seeded on UV sterilized glass slides (75×25 mm). Sixty minutes later, the cells were observed to be attached and the slides were flooded with maintenance media within tissue culture dishes. A total of eight test groups consisting of a minimum of five samples per each condition were created. These test groups consisted of no treatment, Rosiglitazone, GW9662, and PD98059 treatments; all with and without fluid flow.

Twenty-four hours after seeding, the media was changed to fresh media supplemented with the appropriate biochemical factors; 0.5 µM Rosiglitazone, 1 µM GW9662, or untreated (PD98059 is explained later). The groups were then incubated for an additional 48 hours. Cells were stimulated using flow media (DMEM with 1% penicillin-streptomycin and 0.5% fetal bovine serum). After fluid flow, cells were immediately transferred into adipogenic induction media (10 µg/ml insulin, 0.5 mM IBMX, and 1 µM dexamethasone; the same as the stretch tests). Following two days of induction, the media was changed to adipogenic maintenance media (10 µg/ml insulin) and kept for additional eight days.

For ERK activation analysis, C3H10T1/2 MSCs were cultured as described above. Seventy-two hours after seeding, the cells were subjected to fluid flow in serum

starvation media and immediately transferred to ice and harvested for assessment of ERK phosphorylation. This was done using the same protocols as in chapter two. To test the role of ERK in affecting fluid flow control of MSC adipogenesis, cells were seeded and cultured the same but with an one hour treatment with 20 μM PD98059 before flow stimulation. The remainder of the experiment proceeded in the same manner.

Data Collection

To assess adipogenic differentiation, Oil Red O staining was used. As carried out in chapter two for stretched cells, Oil red O stained cells were imaged and the amount of synthesized lipids were quantified by a spectrophotometer. All the lipid staining data points were normalized to untreated static control.

ERK1/2 phosphorylation was measured using western blot analysis. Right after the fluid flow, protein samples were obtained and immunoblotting was performed using the same methods as described in chapter 2. To test the time dependent evolution of ERK1/2 activation as a function of flow stimulation, fluid flow was applied for 10, 20, 30, and 60 minutes and ERK1/2 phosphorylation was measured. The phosphorylation of ERK was quantified by dividing the immunoblot band intensity of the phosphorylated ERK1/2 by that of the total ERK1/2, as in chapter 2.

Analysis of Data

Data was analyzed using InSTAT 3 statistic software. Statistical significance was established using ANOVA followed by post-hoc tests.

Results

Ten days after flow stimulation and subsequent adipogenic induction, lipid accumulation was assessed using Oil Red O staining and quantified. From figure 3-4 A and B, we can see intuitively that fluid flow suppressed lipid accumulation relative to unflowed control. This is evident in figure 3-4 C which shows the quantification of lipid accumulation following extraction by isopropanol. Analysis of the data shows that the differences between the control and fluid flow groups are significant with $p < 0.05$.

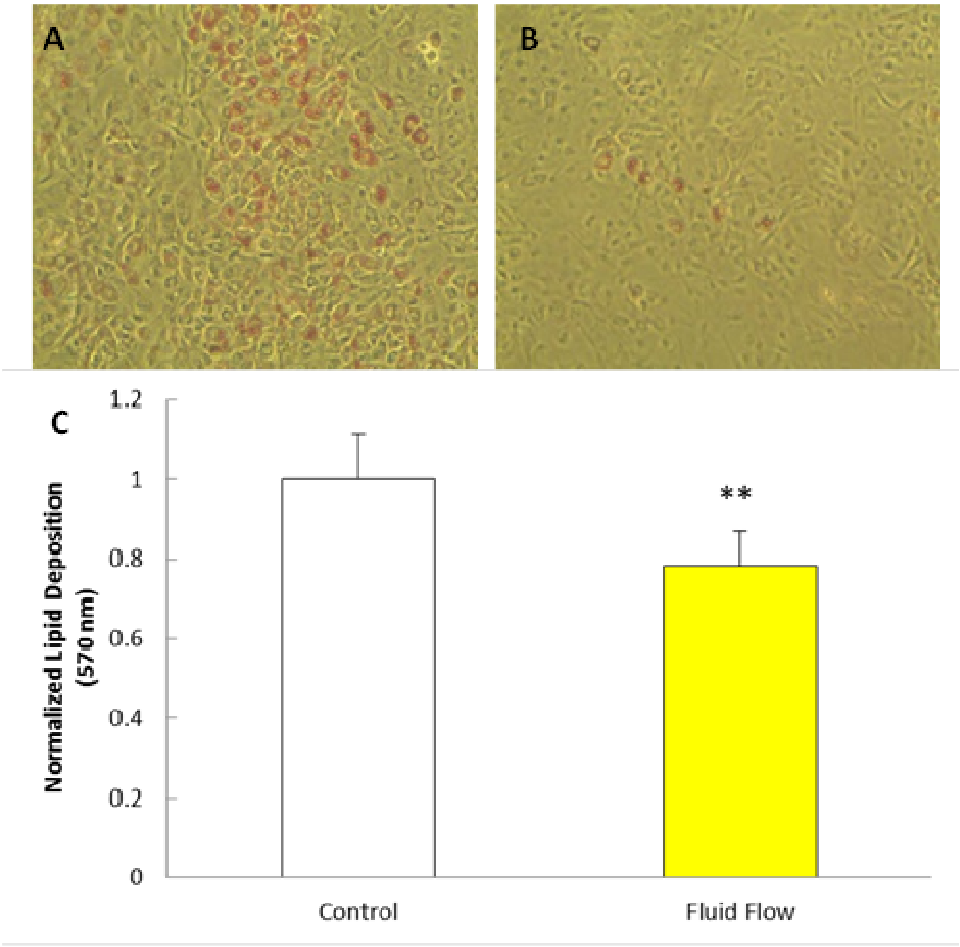

Figure 3-4 Fluid Flow reduces lipid deposition. Oil Red O staining of A) Untreated control and B) Fluid flow groups 10 days post stimulation. C) Quantification of lipid accumulation. Comparison with untreated control at $p < 0.05$ (**)

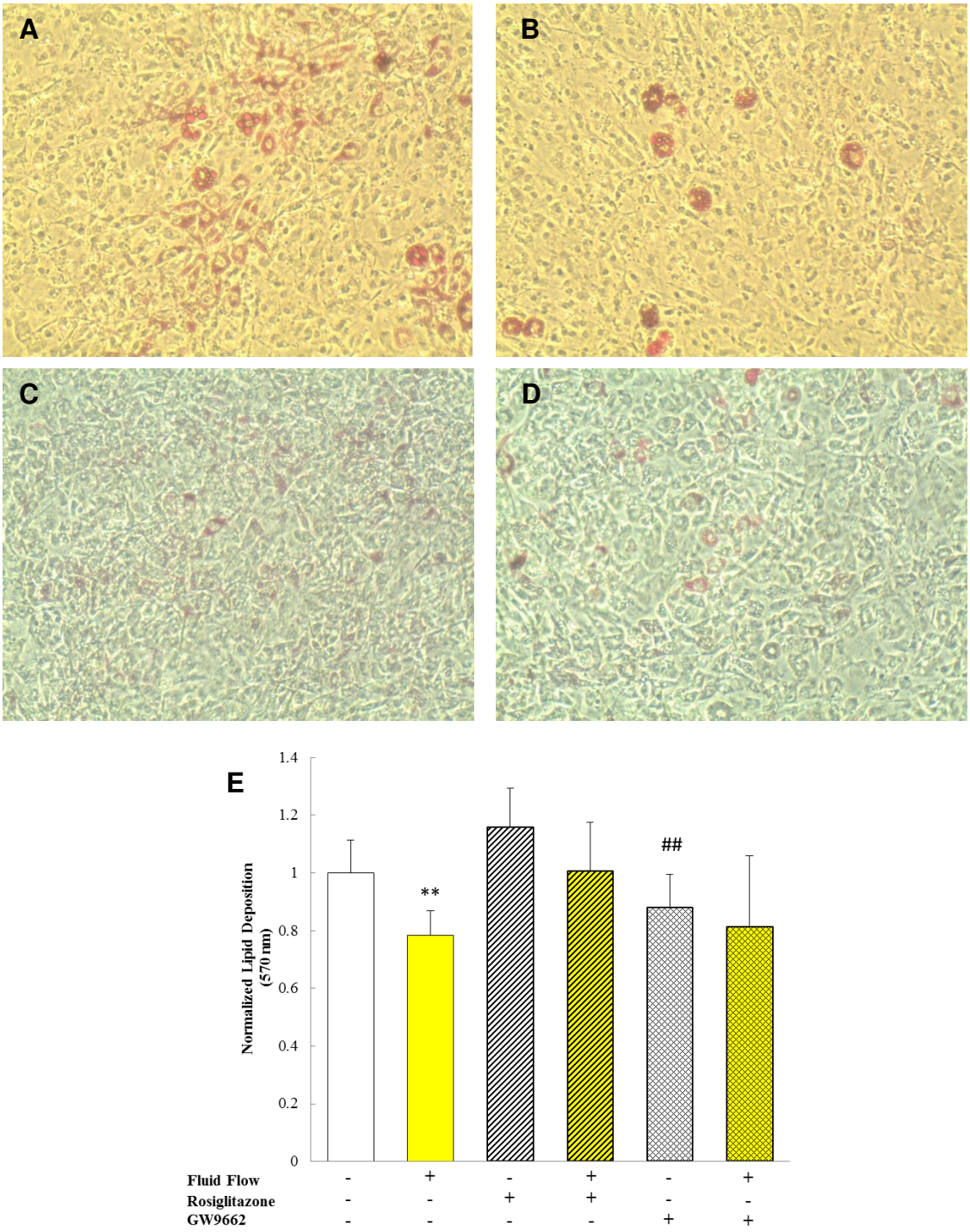

Figure 3-5 Addition of Rosiglitazone and GW9662 modulates fluid flow effect. Oil Red O staining of A,C) Static Control and B,D) Fluid flow groups 10 days post stimulation when treated with Rosiglitazone (A,B) or GW9662 (C,D). E) Quantification of lipid accumulation. Comparison with untreated control at $p < 0.05$ (**) and Rosiglitazone Static Control at $p < 0.01$ (##)

To investigate that fluid flow control of lipid accumulation is dependent on

PPARγ, the experiment was repeated in the presence of Rosiglitazone and GW9662. As expected, the overall level of lipid accumulation was increased by Rosiglitazone and decreased by GW9662 treatment. Even in the presence of Rosiglitazone (PPARγ agonist and thus increasing adipogenesis), the fluid flow stimulation still appeared to work as a suppressor of MSC adipogenesis. However, the decrease by flow did not reach statistical significance. GW9662 (PPARγ antagonist and thus decreasing adipogenesis) induced overall reduction in MSC adipogenesis, and thus flow induced adipogenesis inhibitory effect could hardly be seen.

The time series of ERK phosphorylation as a function of fluid flow is shown in figure 3-6. It is clearly demonstrated that fluid flow stimulation of MSCs induces distinct activation of ERK cascade. The phosphorylation shows a peak at 20 minutes of flow followed by a gradual decrease. This result is comparable to that of the ERK activation by cell stretch, which showed a maximum phosphorylation after 30 min of stretch (figure 2-6). While more systematic studies at varying stretch and fluid flow regimens are required, these data indicate that ERK is activated in MSCs by either cell stretch or fluid flow stimulations. Fine tuning of the stretch and flow regimens may reveal optimal mechanical stimulation conditions to maximize ERK1/2 phosphorylation, thus enabling the triggering of downstream pathways in a most influential manner.

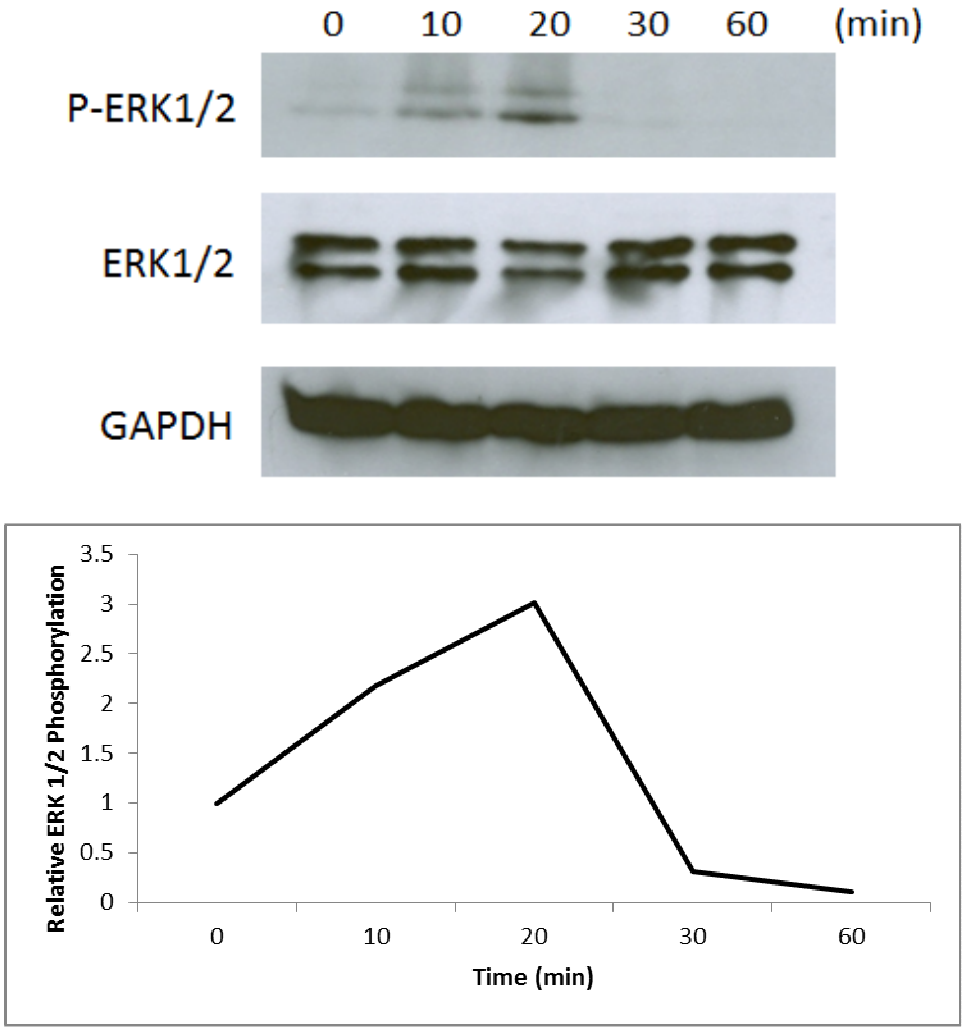

Figure 3-6 Western Blot of ERK 1/2 Phosphorylation after 0, 10, 20, 30 and 60 minutes of Fluid Flow

The potential role of ERK in controlling the fluid flow inhibition of MSC adipogenesis is shown in figure 3-7. If ERK phosphorylation is inhibited by PD98059, MSC adipogenesis is not inhibited by fluid flow. As a result, the flow inhibition of MSC adipogenesis (**: between the first two bars) was not active in the presence of PD98059 (not significant between the third and fourth bars). Note that fluid flowed samples in the absence of PD98059 displayed significantly lower lipid synthesis compared with all three other conditions. All taken together, it may be concluded that fluid flow has a potential to

suppress MSC adipogenesis and this may be mediated by fluid flow induced activation of ERK signaling pathway.

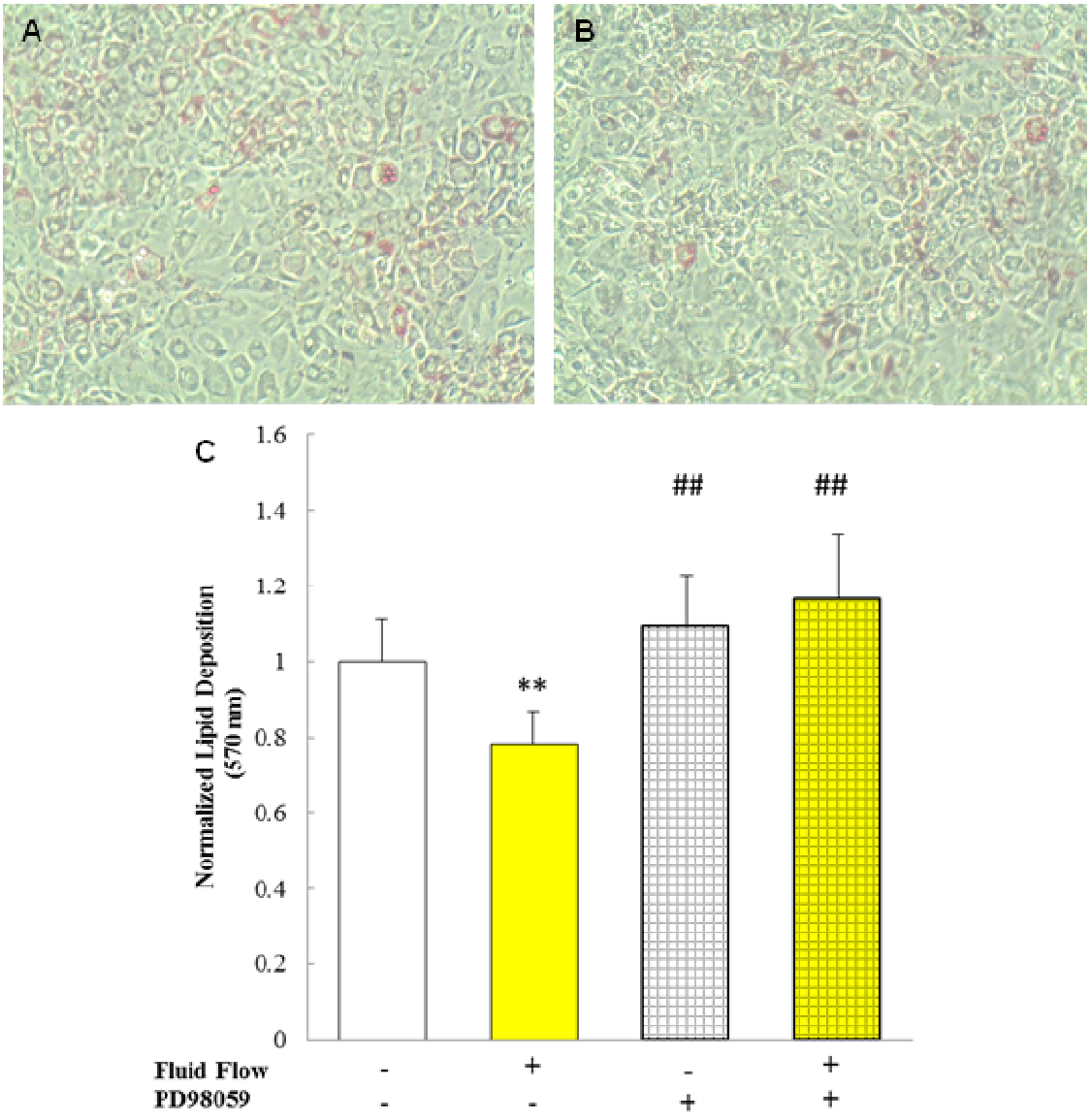

Figure 3-7 Fluid Flow attenuation of MSC Adipogenesis is dependent on ERK phosphorylation. Oil Red O staining of A) PD98059 treated static control and B) PD98059 treated fluid flow groups 10 days post stimulation. C) Quantification of lipid accumulation. Comparison with untreated control at $p < 0.05$ (**) and untreated fluid flow at $p < 0.001$ (##)

Chapter 4 : Discussion

We demonstrated that by subjecting mesenchymal stem cells to mechanical stimulation during pivotal points in early adipogenic differentiation, the effect of biochemical cues can be modulated. In the first section of this study we showed that cell stretching inhibits BMP4 induced MSC adipocytic commitment. This was shown by applying mechanical cell stretch during the BMP4 treatment period. We also confirmed that this is due in some part to stretch activated ERK phosphorylation. The second part of the study demonstrated that oscillatory fluid flow stimulates a similar MSC adipogenesis inhibitory effect. We showed that fluid flow is able to suppress adipogenic differentiation in a PPARγ dependent manner. Such control by fluid flow is also mediated by ERK phosphorylation. In combination, the data strongly suggests that the underlying mechanism of mechanical control of MSC adipogenesis, and in particular, commitment, is related to ERK.

We are the one of the first to demonstrate that cell stretch can exert control of MSC adipogenic commitment prior to induction. This is different than that previously reported by other researchers, which showed that cell stretch during the induction stage could decrease adipogenesis (David, et al., 2007; Tanabe, et al., 2004). It was also recently reported that uniaxial stretch provided during the late stages of adipogenic induction can reduce adipogenesis (Yang, et al., 2012). We demonstrated that by providing mechanical stimulation during the BMP4 mediated MSC commitment stage we could suppress subsequent MSC adipogenesis induced by a hormone cocktail. All combined results indicate that cell stretch is an effective modulator of mesenchymal stem

cell adipogenesis at many if not all stages.

It appears that the inhibitory effect is also dependent on the dynamic nature of cyclic stretch. Levy et al. recently reported that sustained (non-cyclic) stretch had actually the effect of accentuating the adipogenesis (Levy, et al., 2012). These seemingly conflicting results demonstrate the complexity of cell-mechanics interactions and confirm the need for systematic study of cell response to various mechanical stimulation modes and regimens. Studies are also needed to not only compare the effects of fluid flow and stretch as we have done, but also pressure, vibration, and even static physical cue from substrate topography. There also need to be systematic studies of the effect of force/stress magnitude, frequency of loading, axis of loading, the timing of stimulation with regards to both the cell cycle and the stage of differentiation, and rest period between the stimulation.

In the second section of this study we showed that fluid flow exhibits similar inhibitory control of C3H10T1/2 MSC adipogenic differentiation. We showed via lipid accumulation analysis that fluid flow significantly reduced adipogenesis. Next we demonstrated that this was PPARγ dependent by applying Rosiglitazone or GW9662 prior to fluid flow treatment, and observed similar trends when PPARγ was agonized though not significant. On the contrary, when PPARγ was suppressed by GW9662 we could find very little difference in adipogenic commitment.

While we are unable to make direct comparisons between the regulation of C3H10T1/2 MSC adipogenesis by stretch and fluid flow, we can make some broad comparisons. One is that both cell stretch and fluid flow mechanisms are dependent on ERK1/2 phosphorylation. This result may be interesting given the observations of

Gardinier et al. and Maul et al. who found that different mechanical stimulations generate drastically different downstream signal cascades (Gardinier, et al., 2009; Maul, et al., 2011). On the other hand, our data generally agree with results previously published that demonstrate the ERK1/2 is phosphorylated in response to many mechanical cues including fluid flow and mechanical stretch (Tanabe, et al., 2004; Young, et al., 2009).

Note again that we did not use BMP4 in the fluid flow assays as the current fluid flow set up requires too great an amount of BMP4. Even without BMP4, adipogenesis did occur as measured by lipid accumulation, which was suppressed by fluid flow. With BMP4, adipogenesis was rapid and definite, e.g., the cells were obviously accumulating lipids as shown in figure 2-5 and the RT-PCR measurements of key adipogenic genes displayed distinct expression levels. Future studies will be completed to assess all of the adipogenic markers for the case of fluid flow experiments. Further, subsequent studies could probe fluid flow control of BMP4 induced MSC adipogenesis or stretch control of non-BMP4 mediated adipogenesis.

ERK displayed a similar response to both stretch and fluid flow. This may partly be due to flow shear forces generated by the deformation of the membrane during cell stretch. It was shown that in normal operation the Flexcell cell stretch system generates shear forces of 0.1-3.5 Pa on cells (Thompson, et al., 2011). This suggests a need for new experimental methods and protocols to more accurately isolate the stretch and fluid flow parameters. On the other hand, an apparatus that can synergistically combine stretch and fluid flow for inducing enhanced ERK phosphorylation may improve the inhibition of adipogenesis in MSCs.

In both stretch and flow studies, the addition of PD98059, an ERK inhibitor,

suppressed the ability of mechanical stimulation to inhibit MSC adipogenesis. This lends credibility to the theory that ERK plays a pivotal role in mechanical control of adipogenic commitment. This result agrees with the observations of Farmer that PPARγ regulation is dependent on ERK/MEK signaling and cAMP-dependent signaling along with CCAAT/enhancer binding proteins, though this study did not utilize mechanical cell stimulations (Farmer, 2005).

Chapter 5 : Conclusion

In conclusion, we showed that mechanical stimulation plays a pivotal role in the commitment and differentiation of mesenchymal stem cells. Specifically, both stretch and fluid flow stimulations showed a strong potential to decrease MSC adipogenesis. This was demonstrated by (1) cell stretch inhibition of BMP4 modulated upregulation of adipogenic genes and lipid synthesis and (2) fluid flow suppression of PPARγ dependent lipid synthesis, both for C3H10T1/2 MSCs. Importantly, our data demonstrated that ERK1/2 phosphorylation may be significantly involved in both cases, as demonstrated by the observations that under ERK inhibitor mechanical inhibition of MSC adipogenesis was disrupted for both stretch and fluid flow stimulations.

Future research could probe more systematically the mechanical stimulation regimens, for both stretch and fluid flow. Also, fluid flow inhibition of BMP4 induced adipogenic commitment may also be tested. One may also attempt to isolate the effect of membrane and cell deformation from the shear force provided by the media under cell stretch.

We have demonstrated the complex nature of MSC adipogenic commitment, which is dependent on both soluble and mechanical environments, and proposed a potential regulatory mechanism, e.g., ERK, to inhibit MSC adipogenesis and thus to target in the ongoing fight against obesity and obesity related diseases.

References

Akimoto, T., Ushida, T., Myaki, S., Akaogi, H., Tsuchiya, K., Yan, Z., Williams, R., and Tateishi, T. (2005). Mechanical stretch inhibits myoblast-to-adipocyte differentiation through Wnt signaling. Biochemical and Biophysical Research Communications, 329(1), 381-385.

Bandyopadhyay, A., Yadav, P. S., and Prashar, P. (2013). BMP signaling in development and diseases: A pharmacological perspective. Biochemical Pharmacology, 85(7), 857-864.

Benhardt, H., and Cosgriff-Hernandez, E. (2009). The role of mechanical loading in ligament tissue engineering. Tissue Engineering Part B Reviews, 15, 467-475.

Bodle, J., Hanson, A., and Loboa, E. (2011). Adipose-derived stem cells in functional bone tissue engineering: lessons from bone mechanobiology. Tissue Engineering: Part B, 17(3), 195-211.

Bowers, R. R., and Lane, M. D. (2007). A Role for Bone Morphogenetic Protein-4 in Adipocyte Development. Cell Cycle, 6(4), 385-389.

Campbell, J., Lee, D., and Bader, D. (2006). Dynamic compressive strain influences chondrogenic gene expression in human mesenchymal stem cells. Biorhealogy, 43(3-4), 455-470.

Case, N., Sen, B., Thomas, J., Styner, M., Xie, Z., Jacobs, C., and Rubin, J. (2011). Steady and Oscillatory Fluid Flows Produce a Similar Osteogenic Phenotype. Calcified Tissue International, 88(3), 189-197.

Cornier, M.-A., Dabelea, D., Hernandez, T., Lindstrom, R., Steig, A., Stob, N., Van Pelt, R., Wang, H., and Eckel, R. (2008). The Metabolic Syndrome. Endocrine Reviews, 29(7), 777-822.

David, V., Martin, A., Lafage-Proust, M.-H., Malaval, L., Peyroche, S., Jones, D., Vico, L., and Guignandon, A. (2007). Mechanical loading down-regulates peroxisome proliferator-activated receptor gamma in bone marrow stromal cells an favors osteoblastogenesis at the expense of adipogenesis. Endocrinology, 148(5), 2553-2562.

Farmer, S. (2005). Regulation of PPARgamma activity during adipogenesis. International Journal of Obesity, 29, S13-S16.

Finkelstein, E., Trogdon, J., Cohen, J., and Dietz, W. (2009). Annual Medical Spending Attributable to Obesity: Payer and Service-Specific Estimates. Health Affairs, 28(5), w822-w831.

Gardinier, J., Majumdar, S., Duncan, R., and Wang, L. (2009). Cyclic Hydraulic Pressure and Fluid Flow Differentially Modulate Cytoskeleton Re-Organization in MC3T3 Osteoblasts. Cellular and Molecular Bioengineering, 2(1), 133-143.

Ghazanfari, S., Tafazzoli-Shadpour, M., and Shokrgozar, M. (2009). Effects of cyclic

stretch on proliferation of mesenchymal stem cells and their differentiation to smooth muscle cells. Biochemical and Biophysical Research Communications, 388(3), 601-605.

Haasper, C., Jagodzinski, M., Drescher, M., Meller, R., Wehmeier, M., Krettek, C., and Hesse, E. (2008). Cyclic strain induces FosB and initiates osteogenic differentiation of mesenchymal cells. Experimental and Toxicologic Pathology, 59(6), 355-363.

Hamilton, D., and Brunette, D. (2007). The effect of substratum topography on osteoblast adhesion mediated signal transduction and phosphorylation. Biomaterials, 28(10), 1806-1819.

Hogan, B. (1996). Bone morphogenetic proteins: multifunctional regulators of vertebrate development. Genes & Development, 10(13), 1580-1594.

Huang, C.-H., Chen, M.-H., Young, T.-H., Jeng, J.-H., and Chen, Y.-J. (2009). Interactive effects of mechanical stretching and extracellular matrix proteins on initiating osteogenic differentiation on human mesenchymal stem cells. Journal of Cellular Biochemistry, 108(6), 1263-1273.

Kapur, S., Baylink, D., and Lau, K. (2003). Fluid flow shear stress stimulates human osteoblast proliferation and differentiation through multiple interacting and competing signal transduction pathways. Bone, 32(3), 241-251.

Kim, S.-H., Choi, Y., Park, M., Shin, J., Park, K., Kim, S.-J., and Lee, J. (2007). ERK 1/2

activation in enhanced osteogenesis of human mesenchymal stem cells in poly(lactic-glycolic acid) by cyclic hydrostatic pressure. Journal of Biomedical Materials Research Part A, 80A(4), 826-836.

Koike, M., Shimokawa, H., Kanno, Z., Ohya, K., and Soma, K. (2005). Effects of mechanical strain on proliferation and differentiation of bone marrow stromal cell line ST2. Journal of Bone and Mineral Metabolism, 23(3), 219-225.

Lee, J. S., Park, J.-H., Kwon, I. K., and Lim, J. Y. (2011). Retinoic acid inhibits BMP4-induced C3H10T1/2 stem cell commitment. Biochemical and Biophysical Research Communications, 409(3), 550-555.

Lee, J., Ha, L., Park, J.-H., and Lim, J. (2012). Mechanical stretch suppresses BMP4 induction of stem cell adipogenesis via upregulating ERK but not through downregulating Smad or p38. Biochemical and Biophysical Research Communications, 418(2), 278-283.

Lee, J., Suh, J., Park, H., Bak, E., Yoo, Y.-J., and Cha, J.-H. (2008). Heparin-binding epidermal growth factor-like growth factor inhibits adipocyte differentiation at commitment and early induction stages. Differentiation, 76(5), 478-487.

Levy, A., Enzer, S., Shoham, N., Zaretsky, U., and Gefen, A. (2012). Large, but not Small Sustained Tensile Strains Stimulate Adipogenesis in Culture. 40(5), 1052-1060.

Liu, J., Zhao, Z., Li, J., Zou, L., Shuler, C., Zou, Y., Huang, X., Li, M., and Wang, J. (2009). Hydrostatic Pressures Promote Initial Osteodifferentiation With ERK 1/2

Not p38 MAPK Signaling Involved. Journal of Cellular Biochemistry, 107(2), 224-232.

Maul, T., Chew, D., Nieponice, A., and Vorp, D. (2011). Mechanical stimuli differentially control stem cell behavior: morphology, proliferation, and differentiation. Biomechanics and Modeling in Mechanobiology, 10(6), 939-953.

Modica, S., and Wolfrum, C. (2013). Bone morphogenic proteins signaling in adipogenesis and energy homeostasis. Biochimica et Biophysica Acta (BBA) - Molecular and Cell Biology of Lipids, 1831(5), 915-923.

Mullender, M., Dijcks, S., Bacabac, R., Semeins, C., Van Loon, J., and Klein-Nulend, J. (2006). Release of Nitric Oxide, but not Prostaglandin E2, by Bone Cells Depends on Fluid Flow Frequency. Journal of Orthopaedic Research, 24(6), 1170-1177.

Nieponice, A., Maul, T., Cumer, J. M., Soletti, L., and Vorp, D. (2006). Mechanical stimulation induces morphological and phenotypic changes in bone marrow-derived progenitor cells withina a three-dimensional fibrin matrix. Journal of Biomedical Materials Research Part A, 81A(3), 523-530.

Ogden, C., Carroll, M., Kit, B., and Flegal, K. (2012). Prevalence of Obesity in the United States, 2009-2010. NCHS Data Brief, 82, 1-7. Retrieved from Center for Disease Control.

Palaez, D., Arita, N., and Cheung, H. (2012). Extracellular signal-regulated kinase (ERK) dictates osteogenic and/or chondrogenic lineage commitment of mesenchymal

stem cells under dynamic compression. Biochemical and Biophysical Research Communications, 417(4), 1286-1291.

Park, J., Chu, J., Cheng, C., Chen, F., Chen, D., and Li, S. (2004). Differential Effect of Equiaxial and Uniaxial Strain on Mesenchymal Stem Cells. Biotechnology and Bioengineering, 88(3), 359-368.

Ponik, S., Triplett, J., and Pavalko, F. (2007). Osteoblasts and Osteocytes Respond Differently to Oscillatory and Unidirectional Fluid Flow Profiles. Journal of Cellular Biochemistry, 100(3), 794-807.

Qi, M.-C., Hu, J., Zou, S.-J., Chen, H.-Q., Zhou, H.-X., and Han, L.-C. (2008). Mechanical strain induces osteogenic differentiation: Cbfa1 and Ets-1 expression in stretched rat mesenchymal stem cells. International Journal of Oral & Maxillofacial Surgery, 37(5), 453-458.

Radisic, M., Park, H., Gerecht, S., Cannizzaro, C., Langer, R., and Vunjak-Novakovic, G. (2007). Biomimetic approach to cardiac tissue engineering. Philosophical Transacttions of the Royal Society B, 362, 1357-1368.

Riddle, R., Hippe, K., and Bonahue, H. (2008). Chemotransport contributes tothe effect of oscillatory fluid flow on human bone marrow stromal cell proliferation. Journal of Orthopedic Research, 26(7), 918-924.

Salvi, J., Lim, J., and Donahue, H. (2010). Finite Element Analyses of Fluid Flow Conditions in Cell Culture. Tissue Engineering: Part C, 16(4), 661-670.

Shoham, N., and Gefen, A. (2012). Mechanotransduction in adipocytes. Journal of Biomechanics, 45(1), 1-8.

Sumanasinghe, R., Osborne, J., and Loboa, E. (2008). Mesenchymal stem cell-seeded collagen matrices for bone repair: Effects of cyclic tensile strain, cell density, and media conditions on matrix contraction in vitro. Journal of Biomedical Materials Research Part A, 88A(3), 778-786.

Sun, Y., Chen, C., and Fu, J. (2012). Forcing Stem Cells to Behave: A Biophysical Perspecive of the Cellular Microenvironment. Annual Review of Biophysics, 41, 519-542.

Tanabe, Y., Koga, M., Saito, M., Matsunaga, Y., and Nakayama, K. (2004). Inhibition of adipocyte differentiation by mechanical stretching through ERK-mediated downregulation of PPARgamma. Journal of Cell Science, 117(16), 3605-3614.

Tang, Q.-Q., Otto, T., and Lane, M. (2003). Mitotic clonal expansion: A synchronous process required for adipogenesis. Proceedings of the National Academy of Sciences, 100(1), 44-49.

Thompson, M., Abercrombie, S., Ott, C.-E., Bieler, F., Duda, G., and Ventikos, Y. (2011). Quantification and significance of fluid shear stress field in biaxial cell stretching device. Biomechanics and Modeling in Mechanobiology, 10(4), 559-564.

Urist, M. (1965). Bone: Formation by autoinduction. Science, 150(3698), 893-899.

Wadhwa, S., Choudhary, S., Voznesensky, M., Epstein, M., Raisz, L., and Pilbeam, C.

(2002). Fluid flow induces COX-2 expression in MC3T3-E1 osteoblasts via a PKA signaling pathway. Biochemical and Biophysical Research Communications, 297(1), 46-51.

Yang, X., Cai, X., Wang, J., Yuan, Q., Gong, P., and Lin, Y. (2012). Mechanical stretch inhibits adipogenesis and stimulates osteogenesis of adipose stem cells. Cell Proliferation, 45(2), 158-166.

Yang, X., Gong, P., Lin, Y., Zhang, L., Li, X., Quan, Y., Tan, Z., Wang, Y., Man, Y., and Tang, H. (2010). Cyclic tensile stretch modulates osteogenic differentiation of adipose-derived stem cells via the BMP-2 pathway. Archives of Medical Science, 6(2), 152-159.

Young, S. R., Gerard-O'Riley, R., Kim, J.-B., and Pavalko, F. (2009). Focal Adhesion Kinase Is Important for Fluid Shear Stress-Induced Mechanotransduction in Osteoblasts. Journal of Bone and Mineral Research, 24, 411-424.

Yu, Z., Wright, J., and Hausman, G. (1997). Preadipocyte Recruitment in Stromal Vascular Cultures After Bepletion of Committed Preadipocytes by Immunocytotoxicity. Obesity Research, 5(1), 9-15.